Prediction of the Fermi surface as a test of density-functional approximations to the self-energy*†

S. B. Nickerson and S. H. Vosko
Department of Physics and Erindale College, University of Toronto, Toronto, Ontario, Canada M5S 1A7
(Received 12 May 1976)

Prediction of alkali-like Fermi surfaces is used as a test of the local and nonlocal density-functional approximations to the electron self-energy proposed by Sham and Kohn. This test is carried out in a Hartree-Fock (HF) model system where a Yukawa interaction between the electrons is used in order to simulate screening. The Fermi surfaces resulting from the density-functional approximations to the exchange term are compared to the exact HF Fermi surface. It is found that the local and nonlocal approximations produce Fermi surfaces which are too distorted and too spherical, respectively. This reconciles previous local and nonlocal Fermi-surface calculations in the alkali metals with known experimental results. It is shown that the Fermi surface is much more sensitive to the approximations made to the self-energy than other properties such as the density and chemical potential, which we find are treated with sufficient accuracy by the local approximation.

I. INTRODUCTION

First-principles Fermi-surface predictions seem to be very sensitive to the form with which one approximates the self-energy[1-9] and such predictions generally do not agree with experiment. For example, in the alkali metals,[1-3,6-9] the distortions from sphericity, resulting from a local approximation to the self-energy, are usually much too large.

The purpose of this paper is to examine this sensitivity of Fermi-surface prediction and in particular to study two approximations to the electron self-energy which are based on density-functional theory[10-12] and homogeneous-electron-gas results. The first approximation, which is local, was introduced by Kohn and Sham[11] who showed that it could be used to calculate the electron density and ground-state energy. In a subsequent paper, Sham and Kohn[10] argue that this local approximation [hereafter called the local density-functional (LDF) approximation—see (2.16)] can also be used to predict the chemical potential and Fermi surface. Sham and Kohn introduce another approximation, given by (2.12), which is nonlocal [we shall call this the nonlocal density-functional (NLDF) approximation]. Unlike the LDF approximation, which should only be used to calculate the above mentioned properties, the NLDF approximation can be used to approximate the Green's function and therefore any property of the system can be calculated.

Rasolt and Vosko[13,14] have done a model calculation in a simple (alkalilike) system. They compared the results of the LDF and NLDF approximations and found the NLDF Fermi surface was much more spherical than the LDF Fermi surface. They have shown that LDF theory is not a good approximation to NLDF theory if used to predict the Fermi surface. A similar calculation was done for lithium.[1] Again the NLDF approximation produced a much more spherical Fermi surface than the equivalent LDF approximation. The above results indicate that the nonlocal aspect of the self-energy is important in reducing the Fermi surface distortions from those predicted by LDF theory and this trend is in qualitative agreement with experiment for the alkali metals.[1-3,5-9] However, the quantitative aspects of the NLDF approximation have yet to be determined since the Fermi surface of lithium has not been measured with sufficient accuracy.[15-17]

Therefore, we wish to investigate in detail the accuracy of the LDF and NLDF approximations to the self-energy in predicting the Fermi surface. This is accomplished by having calculated the exact results of a self-consistent Hartree-Fock (HF) model with which to compare the results of LDF and NLDF approximations to the exchange term. These exact results are used to examine the sensitivity of the predicted Fermi surface to the nature of the approximations compared to the sensitivity of the predicted chemical potentials and electron densities. In order to simulate the effects of screening in a metal, we allow the electrons to interact via a Yukawa interaction with variable strength and range. Results are presented for three sets of Yukawa parameters, each defining an exchange term which has some of the screening characteristics of a realistic self-energy.

Tong and Sham[18] have compared HF electron densities in atoms with those produced by the LDF approximation and have found good agreement.

We compare the electron densities and the chemical potentials of LDF and NLDF calculations in a metalliclike system with the exact HF results and find similar agreement.

The density-functional formalism[10-12] leads to approximations (such as the NLDF approximation) of the self-energy which depend only on the electron density and not completely on the Green's function. Such systems can be solved either self-consistently or non-self-consistently using the LDF charge densities to construct the self-energy. Using the NLDF and LDF approximations to the HF model, a comparison is made of the Fermi surfaces corresponding to both of these alternatives.

II. APPROXIMATIONS TO THE SELF-ENERGY

The quasiparticle spectrum (and hence the Fermi surface) and the electron density can be determined from the Green's function $G(\vec{r},\vec{r}';E)$, which is a solution to Dyson's equation[10] (the spin indices are included in $\vec{r}$):

$$[-E-\nabla^2+\phi(\vec{r})]G(\vec{r},\vec{r}';E)+\int d\vec{r}''\,M(\vec{r},\vec{r}'';E)G(\vec{r}'',\vec{r}';E)=-\delta(\vec{r}-\vec{r}'), \tag{2.1}$$

$$\phi(\vec{r})=V_{\text{ext}}(\vec{r})+V_H(\vec{r}), \tag{2.2}$$

$$V_H(\vec{r})=\int d\vec{r}'\,n(\vec{r}')U(|\vec{r}-\vec{r}'|). \tag{2.3}$$

Atomic units are used with all energies in rydbergs. $M(\vec{r},\vec{r}';E)$ is the self-energy. $V_{\text{ext}}(\vec{r})$ is the external (periodic) potential with bcc symmetry. $U(|\vec{r}-\vec{r}'|)$ is the interparticle interaction and $V_H(\vec{r})$ is the Hartree term with $n(\vec{r})$ the electron density.

The HF approximation of $M(\vec{r},\vec{r}';E)$ is sufficient for a study of the LDF and NLDF approximations since the exchange term is nonlocal and can be made to simulate a realistic self-energy by allowing the electrons to interact by means of a Yukawa interaction. It is a long and difficult computation to find the Fermi surface of a HF metalliclike system. However, an exact solution is possible because the exchange term is both E independent and Hermitian. In contrast the self-energy in the self-consistent inhomogeneous random-phase approximation[19] (RPA) is both E dependent and non-Hermitian. This computation appears to be out of reach at the present time.

The HF Green's function can be constructed from the solutions to the following equation[20]:

$$[-\nabla^2+\phi(\vec{r})]\psi_{\nu\vec{k}}(\vec{r})+\int d\vec{r}'\,M_x(\vec{r},\vec{r}')\psi_{\nu\vec{k}}(\vec{r}')=\epsilon_{\nu\vec{k}}\psi_{\nu\vec{k}}(\vec{r}), \tag{2.4}$$

where $\vec{k}$ is the wave vector, and ν is the band index of $\psi_{\nu\vec{k}}$ and $\epsilon_{\nu\vec{k}}$, the wave functions and eigenvalues from which the Green's function is calculated. We are considering one atom per unit cell and will often use $\epsilon_{\vec{k}}$ and $\psi_{\vec{k}}$ which will be understood to mean $\epsilon_{1\vec{k}}$ and $\psi_{1\vec{k}}$. $M_x(\vec{r},\vec{r}')$ is the exchange term given by

$$M_x(\vec{r},\vec{r}')=-U(|\vec{r}-\vec{r}'|)\sum_{\vec{k}'}\Theta(\mu-\epsilon_{\vec{k}'})\times\psi_{\vec{k}'}(\vec{r})\,\psi^*_{\vec{k}'}(\vec{r}'); \tag{2.5}$$

μ is the chemical potential and Θ is the unit step function. The sum over $\vec{k}'$ does not include a sum over spin. The electron density is

$$n(\vec{r})=2\sum_{\vec{k}'}\Theta(\mu-\epsilon_{\vec{k}'})|\psi_{\vec{k}'}(\vec{r})|^2. \tag{2.6}$$

To simulate screening we use a Yukawa-type potential, for the interparticle interaction, with variable strength and range

$$U(|\vec{r}-\vec{r}'|)=2U_0e^{-\xi|\vec{r}-\vec{r}'|}/|\vec{r}-\vec{r}'|. \tag{2.7}$$

We choose different sets of Yukawa parameters, U_0 and ξ, such that M_x simulates different screening characteristics of a real metal. We are guided by electron gas theory in making these choices. Let $M_h(\vec{r}-\vec{r}';E;n(r_s))$ be the self-energy of a homogeneous Coulomb electron gas of density $n(r_s)=(\frac{4}{3}\pi r_s^3)^{-1}$. A realistic approximation to this is

$$M_h(\vec{r}-\vec{r}';E;n(r_s))\simeq M_h^{\text{RPA}}(\vec{r}-\vec{r}';\mu_h(n(r_s));n(r_s)), \tag{2.8}$$

where M_h^{RPA} consists of the exchange term plus the RPA term with E on the Fermi surface, i.e., $E=\mu_h(n(r_s))$, the chemical potential. This choice of E guarantees that M_h^{RPA} is real. It is convenient to use the Fourier transform of M_h^{RPA} defined by

$$M_h^{\text{RPA}}(\vec{r}-\vec{r}';\mu_h(n(r_s));n(r_s))=\int\frac{d\vec{P}}{(2\pi)^3}M_h^{\text{RPA}}(\vec{P},\mu_h(n(r_s));n(r_s))\,e^{i\vec{P}\cdot(\vec{r}-\vec{r}')}. \tag{2.9}$$

An analytic expression for $M_h^{\text{RPA}}(\vec{P},\mu_h(n(r_s));n(r_s))$ and figures with $r_s=2,3,4$ can be found in Rasolt and Vosko.[13,14] The self-energy of a Yukawa electron gas is, in the HF approximation,

$$M_h^{XY}(\vec{P}, n(r_s)) = -2\frac{U_0 k_F(r_s)}{\pi}\left\{1 - \frac{1-X^2+X_\xi^2}{4X}\ln\left(\frac{(1-X)^2+X_\xi^2}{(1+X)^2+X_\xi^2}\right) - X_\xi\left[\tan^{-1}\left(\frac{1-X}{X_\xi}\right)+\tan^{-1}\left(\frac{1+X}{X_\xi}\right)\right]\right\}, \quad (2.10)$$

with

$$k_F(r_s) = [3\pi^2 n(r_s)]^{1/3}, \qquad X = P/k_F(r_s); \quad X_\xi = \xi/k_F(r_s). \quad (2.11)$$

U_0 and ξ are adjusted so that $M_h^{XY}(\vec{P}, n(r_s))$ behaves as closely as possible to $M_h^{\mathrm{RPA}}(\vec{P}, \mu_h(n(r_s)); n(r_s))$. In this way $M_h^{XY}(\vec{P}, n(r_s))$ is able to simulate realistic screening properties of a homogeneous system. This similarity is expected to carry over to an inhomogeneous system.

In Figs. 1–3, M_h^{RPA} and M_h^{XY} are compared at $r_s = 2, 3, 4$ for three different sets of Yukawa parameters (Table I). Set A (Fig. 1) is chosen so that M_h^{XY} and M_h^{RPA} are equal at $P = 0$ and very similar at $r_s = 3$ for all P. However, the functional behavior of M_h^{XY}, with respect to r_s, is different from that of M_h^{RPA} for $P < 1.5k_0$ (k_0 is the free-electron Fermi radius). With P above this point the M_h^{XY} curves for different r_s have crossed over and the functional behavior of M_h^{XY} and M_h^{RPA} is the same although the values of each at a given r_s are somewhat different. If U_0 and ξ are adjusted so that M_h^{XY} and M_h^{RPA} have the same value and slope at $P = k_0$, with $r_s = 3$, then set B (Fig. 2) is obtained. M_h^{XY} falls off more steeply with P than M_h^{RPA}, has approximately the correct shape at $r_s = 3$ but has a different functional behavior with respect to r_s for $P < k_0$. With $P > k_0$, M_h^{XY} again has the same functional behavior as M_h^{RPA}. The Yukawa parameters for set C are chosen so that M_h^{XY} and M_h^{RPA} are equal (but do not have equal slopes) at $P = k_0$ and $r_s = 3$ (Fig. 3). We also require that M_h^{XY} have the same functional behavior with respect to r_s as does M_h^{RPA}, throughout the entire range of P. But M_h^{XY} falls off more steeply with P than M_h^{RPA} and in general M_h^{XY} does not agree in value with M_h^{RPA}.

As mentioned earlier, each set of parameters leads to a $M_h^{XY}(P, n(r_s))$ with some, but not all, of the features of a realistic self-energy. Note that if the Thomas-Fermi values ($U_0 = 1$ and $\xi^2 = 0.815$ at $r_s = 3$) are used, the resulting M_h^{XY} is very different from M_h^{RPA}. Each set of Yukawa parameters has been chosen so that M_h^{XY} has closest agreement with M_h^{RPA} at $r_s = 3$ because all our results (Fermi surfaces, etc.) for the inhomogeneous system are obtained with $r_s = 3$. This will be seen to be significant in connection with the NLDF approximation.

For electrons with slowly varying density, M can be approximated as follows (Sham and Kohn[10]):

$$M(\vec{r}, \vec{r}'; E) \simeq M_h(\vec{r} - \vec{r}'; E - \mu + \mu_h(n(\vec{r}_0)); n(\vec{r}_0)). \quad (2.12)$$

The approximation (2.12) is the NLDF approximation where $\vec{r}_0 = \frac{1}{2}(\vec{r} - \vec{r}')$. M_h is the self-energy and μ_h is the chemical potential of a uniform electron gas with density $n(\vec{r}_0)$. Recalling that M_x is independent of E, the corresponding NLDF approximation to M_x is given by

$$M_x(\vec{r}, \vec{r}') \simeq M_x^{\mathrm{NL}}(\vec{r} - \vec{r}'; n(\vec{r}_0)), \quad (2.13)$$

where

$$M_x^{\mathrm{NL}}(\vec{P}, n(\vec{r}_0)) = M_h^{XY}(\vec{P}, n(\vec{r}_0)); \quad (2.14)$$

i.e., $M_x^{\mathrm{NL}}(\vec{P}, n(\vec{r}_0))$ is given by (2.10) and (2.11) with $k_F(r_s)$ replaced by

$$k_F(\vec{r}_0) = [3\pi^2 n(\vec{r}_0)]^{1/3}. \quad (2.15)$$

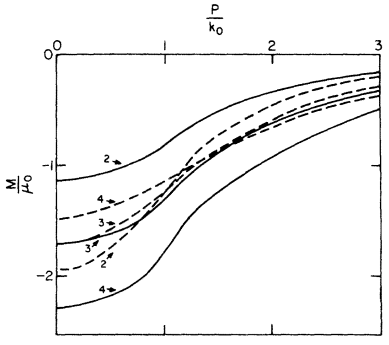

FIG. 1. Solid line is $M_h^{\mathrm{RPA}}(\vec{P}, \mu_h(n(r_s)); n(r_s))$ of (2.9) and the dashed line is $M_h^{XY}(\vec{P}, n(r_s))$ of (2.10) with Yukawa parameters of set A in Table I. The r_s values are beside each curve. $k_0 = k_F(r_s)$ of (2.11) and $\mu_0 = k_0^2$.

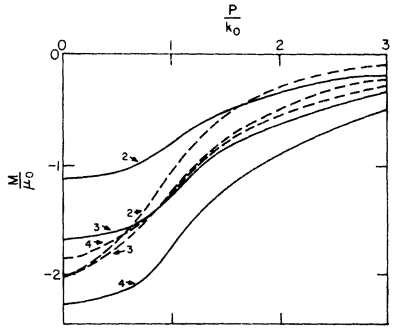

FIG. 2. Dashed line for Yukawa parameters of set B. See Fig. 1.

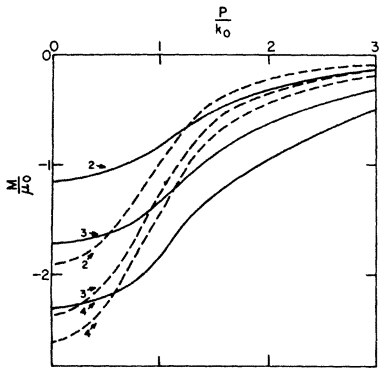

FIG. 3. Dashed line for Yukawa parameters of set C. See Fig. 1.

The significance of choosing the Yukawa parameters such that M_h^{XY} has closest agreement with M_h^{RPA} at $r_s=3$ (the r_s of the inhomogeneous system) is now clear. The NLDF Yukawa exchange term for the inhomogeneous system most closely resembles M_h^{RPA} at the average density.

For electrons having energies equal to the chemical potential, Sham and Kohn[10] give a local approximation to M,

$$M(\vec{r},\vec{r}';\mu)\simeq\mu_{xc}(n(\vec{r}))\,\delta(\vec{r}-\vec{r}')\,. \tag{2.16}$$

The above approximation is the LDF approximation with

$$\mu_{xc}(n(\vec{r}))=\frac{d}{dn}\left[n(\vec{r})\epsilon_{xc}(n(\vec{r}))\right], \tag{2.17}$$

and $\epsilon_{xc}(n(\vec{r}))$ is the exchange and correlation energy per electron of a uniform electron gas of density $n(\vec{r})$. The results of approximation (2.16) can be used to obtain the Fermi surface,[10] chemical potential,[10] electron density,[11] and ground-state energy.[11] The LDF approximation to M_x is

$$M_x(\vec{r},\vec{r}')\simeq M_x^L(n(\vec{r}))\delta(\vec{r}-\vec{r}')\,, \tag{2.18}$$

where

$$M_x^L(n(\vec{r}))=-2\,\frac{U_0 k_F(\vec{r})}{\pi}\times\left[1-Z_\xi\tan^{-1}\left(\frac{2}{Z_\xi}\right)+\frac{Z_\xi^2}{4}\ln\left(\frac{4+Z_\xi^2}{Z_\xi^2}\right)\right], \tag{2.19}$$

where $k_F(\vec{r})=[3\pi^2 n(\vec{r})]^{1/3}$ and $Z_\xi=\xi/k_F(\vec{r})$.

In summary, (2.4) and (2.5) lead to the exact Fermi surface, while the approximations to (2.5), defined by (2.13) and (2.18), lead to the NLDF and LDF approximate Fermi surfaces.

TABLE I. Yukawa parameters. r_{nn} is the nearest-neighbor distance.

Set No.	U_0	ξ^2	$1/\xi r_{nn}$
A	5.05	0.561	0.253
B	3.58	0.261	0.371
C	2.11	0.05	0.848

III. DESCRIPTION OF THE MODEL

The external potential is chosen to be a pseudopotential

$$V_{ext}(\vec{r})=\sum_{\vec{G}} e^{i\vec{G}\cdot\vec{r}}V_{ext}(G)\,. \tag{3.1}$$

For the results given in Sec. V, the parameters are

$$r_s=3,\quad V_{ext}(G_{110})=-0.12,\quad V_{ext}(G>G_{110})=0\,. \tag{3.2}$$

We have found that our conclusions (Sec. V) do not depend on the sign of $V_{ext}(G_{110})$ or on the details of $V_{ext}(G>G_{110})$.

Since a pseudopotential is being used, it is natural to expand the wave function in terms of plane waves

$$\psi_{\nu\vec{k}}(\vec{r})=\sum_{\vec{G}} C_{\vec{G}}(\nu\vec{k})\frac{e^{i(\vec{k}+\vec{G})\cdot\vec{r}}}{\sqrt{\Omega}}\,, \tag{3.3}$$

where Ω is the crystal volume. With this expansion, the LDF, NLDF, and HF operator equations can be replaced by equivalent matrix equations with all equations having the same form, the matrix elements being

$$\Gamma_{\vec{G},\vec{G}'}(\vec{k})=|\vec{k}+\vec{G}|^2\delta_{\vec{G},\vec{G}'}+V_{ext}(\vec{G}-\vec{G}')+n(\vec{G}-\vec{G}')U(\vec{G}-\vec{G}')+M(\vec{G},\vec{G}';\vec{k})\,, \tag{3.4}$$

with $\epsilon_{\vec{k}}$ the eigenvalues and $C_{\vec{G}}(\vec{k})\equiv C_{\vec{G}}(1\vec{k})$ the eigenvectors. M is either the LDF, NLDF, or HF self-energy given below. $n(G)$ is the Fourier transform of $n(\vec{r})$:

$$n(\vec{r})=\sum_{\vec{G}} e^{i\vec{G}\cdot\vec{r}}n(\vec{G}), \tag{3.5}$$

and $U(q)$ is the Fourier transform of $U(r)$:

$$U(q)=8\pi U_0/(q^2+\xi^2)\,. \tag{3.6}$$

In terms of the self-consistent $\epsilon_{\vec{k}}$ and $C_{\vec{G}}(\vec{k})$, it is easily seen that

$$n(\vec{G})=\frac{2}{\Omega}\sum_{\vec{k}'}\Theta(\mu-\epsilon_{\vec{k}'})\sum_{\vec{G}'} C_{\vec{G}'}(\vec{k}')C^*_{\vec{G}'+\vec{G}}(\vec{k}')\,. \tag{3.7}$$

To solve the HF problem according to (2.5) and (3.3), $M(\vec{G},\vec{G}';\vec{k})$ in (3.4) is replaced by

$$M_x(\vec{G},\vec{G}';\vec{k}) = -\frac{1}{\Omega}\sum_{\vec{k}'}\Theta(\mu-\epsilon_{\vec{k}'}) \times\sum_{\vec{G}''} C_{\vec{G}''}(\vec{k}')\,C^{*}_{\vec{G}''+\vec{G}-\vec{G}'}(\vec{k}') \times U(\vec{k}-\vec{k}'+\vec{G}'-\vec{G}''). \quad (3.8)$$

The LDF approximation to the exchange term, $M_x(\vec{G},\vec{G}';\vec{k})$, is $M_x^{L}(\vec{G}-\vec{G}')$ [see (2.19)], where

$$M_x^{L}(n(\vec{r})) = \sum_{\vec{G}} e^{i\vec{G}\cdot\vec{r}} M_x^{L}(\vec{G}). \quad (3.9)$$

Because of the $\vec{r}_0$ dependence, the transform of M_x^{NL} of (2.13) is slightly more complicated.[12] In solving the NLDF problem, $M(\vec{G},\vec{G}';\vec{k})$ in (3.4) is replaced by $M_x^{NL}(\vec{k}+\frac{1}{2}(\vec{G}+\vec{G}'),\vec{G}-\vec{G}')$, where

$$M_x^{NL}(\vec{P},n(\vec{r}_0)) = \sum_{\vec{G}} e^{i\vec{G}\cdot\vec{r}_0} M_x^{NL}(\vec{P},\vec{G}). \quad (3.10)$$

Although it is not obvious from (3.8), $M_x(\vec{G},\vec{G}';\vec{k})$ depends on the same two variables as $M_x^{NL}(\vec{k}+\frac{1}{2}(\vec{G}+\vec{G}'),\vec{G}-\vec{G}')$, i.e., $\vec{k}+\frac{1}{2}(\vec{G}+\vec{G}')$ and $\vec{G}-\vec{G}'$. In contrast $M_x^{L}(\vec{G}-\vec{G}')$ is independent of $\vec{k}$.

IV. COMPUTATIONAL TECHNIQUES

The HF computer program is very long running unless precautions are taken against inefficiency. Two separate techniques have been developed which reduce the running time by more than an order of magnitude over traditional methods. The first technique involves efficient evaluation of sums which occur in the exchange term. The second technique is a numerical method of evaluating two-dimensional integrals with integrands having cubic symmetry.[21]

The exchange term (3.8) [the analysis given below also applies to the charge density, (3.7)] can be rewritten

$$M_x(\vec{G},\vec{G}';\vec{k}) = -\frac{1}{(2\pi)^3}\int_{1/48} d\vec{k}'\,\Theta(\mu-\epsilon_{\vec{k}'})\sum_{\vec{G}''} C_{\vec{G}''}(\vec{k}')\sum_{\hat{R}} C^{*}_{\vec{G}''+\hat{R}\vec{G}_\eta}(\vec{k}')\,U(\hat{R}\hat{R}_\tau(\vec{k}+\vec{G}')-(\vec{k}'+\vec{G}'')). \quad (4.1)$$

To arrive at (4.1),

$$\frac{1}{\Omega}\sum_{\vec{k}}\Theta(\mu-\epsilon_{\vec{k}'})\cdots$$

is replaced by

$$\frac{1}{(2\pi)^3}\int_{1/48} d\vec{k}'\,\Theta(\mu-\epsilon_{\vec{k}'})\sum_{\hat{R}}\cdots,$$

where $\sum_{\hat{R}}\cdots$ is a sum of symmetry operations and

$$\int_{1/48} d\vec{k}'\,\Theta(\mu-\epsilon_{\vec{k}'})\cdots$$

is an integral over the irreducible $\frac{1}{48}$ under the self-consistent Fermi surface. $\hat{R}_\tau$ and $\vec{G}_\eta$ are related by

$$\hat{R}_\tau(\vec{G}-\vec{G}') = \vec{G}_\eta. \quad (4.2)$$

$\vec{G}_\eta$ is a (constant) member of the shell to which $\vec{G}-\vec{G}'$ belongs, chosen arbitrarily. For example, $\vec{G}_1=(0,0,0)(2\pi/a_L)$, $\vec{G}_2=(1,1,0)(2\pi/a_L)$, etc., where a_L is the lattice spacing. The basis set $\{\vec{G}''\}$ is $\vec{k}$ independent consisting of shells around a representative $\vec{k}$ value. The introduction of $\vec{G}_\eta$ makes feasible the precalculation and storage of the values of $\vec{G}''+\hat{R}\vec{G}_\eta$ which belong to $\{\vec{G}''\}$. As an example, consider a calculation using 28 basis functions. Of the original $\sim 5\times10^5$ values of $\vec{G}''+\hat{R}(\vec{G}-\vec{G}')$, there are 10 752 possible values of $\vec{G}''+\hat{R}\vec{G}_\eta$ with only 3742 of these belonging to $\{\vec{G}''\}$. The amount of storage needed has, therefore, been reduced by a factor of 50. This precalculation has the effect of reducing the overall running time of the program by a factor of 6. Further efficiency is gained after noting that many values of $C_{\vec{G}''}C^{*}_{\vec{G}''+\hat{R}\vec{G}_\eta}$ are likely to be small. Such terms can be predetermined and need not be considered in the evaluation of $M_x(\vec{G},\vec{G}';\vec{k})$. For this work 20 basis functions gave convergence.

Efficiency in evaluation of the integral in (4.1) is vital because the running time of the program is almost proportional to the number of $\vec{k}$ points sampled. The integrand of (4.1) has full cubic symmetry and so the most efficient method of evaluation of the angular integral is the use of the two-dimensional Gaussian formulas for integrands of cubic symmetry.[21] It is found, for the parameters used, that a four direction formula is sufficient. If we consider a cubic harmonic[22] expansion of the integrand of (4.1), having done the k' integration, with expansion coefficients $a_{l,r}$, where l is the angular momentum quantum number and r distinguishes between linearly independent cubic harmonics of the same l, the first term in the error expansion is proportional to $a_{18,2}$ for this four-point formula.[21] Using $(k')^3$ as the variable, the k' integration required three sample points for a total of 12 sample points to do the $\vec{k}'$ integration. This was carefully checked to be certain that $M_x(\vec{G},\vec{G}';\vec{k})$ was evaluated accurately.

Another use of the two-dimensional Gaussian formulas is in finding the volume under a constant

energy surface, which is needed when iterating to find the Fermi energy and thus the Fermi surface. The energy is adjusted until the volume enclosed is equal to $\frac{4}{3}\pi k_0^3$, where k_0 is the free-electron Fermi radius. Having obtained the Fermi energy, the Fermi radius $k_F(\Omega)$ in the Gaussian directions is also known. From these values the cubic harmonic expansion coefficients of $k_F(\Omega)$ can be obtained by the numerical evaluation of projection integrals.[21] Again it is found that a four-direction formula is sufficient.

V. RESULTS AND CONCLUSIONS

We present the Fermi surfaces, for the Yukawa parameters listed in Table I, in Figs. 4–6. It is clear that the values of U_0 and ξ greatly affect the relative distortions of the LDF, NLDF, and HF Fermi surfaces. One trend, which is independent (for the range of variation considered) of the functional behavior of M_x^{NL}, is evident: the presence of nonlocality in the self-energy (HF and NLDF) produces a Fermi surface which is always more spherical than the LDF Fermi surface. It is important to note that the exact HF result always lies between the LDF and NLDF Fermi surfaces. These facts imply that it is the nature of the NLDF and LDF approximations to produce this bracketing of the HF Fermi surface. The Yukawa exchange term associated with each set of Yukawa parameters has some of the characteristics of a realistic self-energy so it is to be expected that for a metal NLDF and LDF calculations would predict Fermi surfaces which are too spherical and too distorted, respectively. These results are consistent with theory and experiment in the alkali metals. Except for Na, whose distortions are extremely small, the maximum distortions predicted from local potentials[1-3,5-9] are considerably larger than the maximum distortions of the Fermi surface[5,15-17]. In Li both LDF and NLDF predictions of the Fermi surface have been made using a realistic approximation to the self-energy.[1] At the time the NLDF calculation was expected to predict the Fermi surface of Li more accurately than the LDF calculation. However, it produced a Fermi surface which was more spheri-

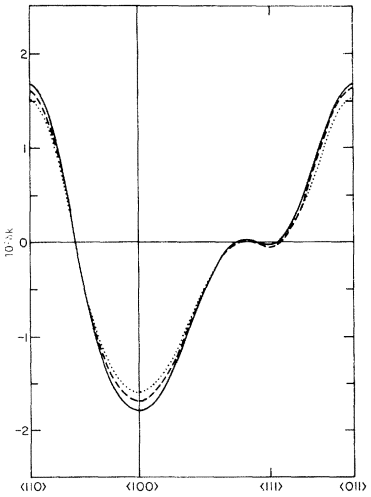

FIG. 4. Radial distortions $\delta k = (k_F - k_0)/k_0$ for k_F in the indicated directions. The solid line is the LDF result, the dashed line is the HF result, and the dotted line is the NLDF result. Yukawa parameter set *A* of Table I is used.

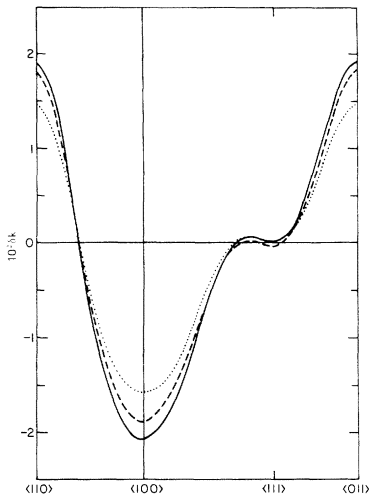

FIG. 5. Radial distortions for Yukawa parameter set *B*. See Fig. 4.

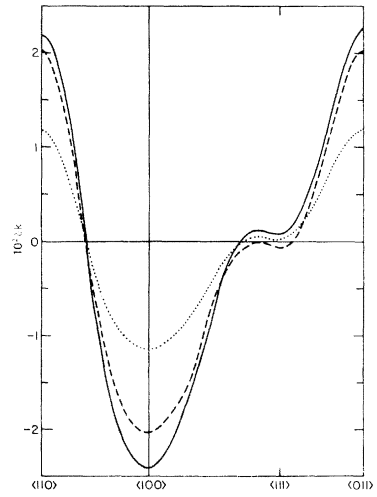

FIG. 6. Radial distortions for Yukawa parameter set *C*. See Fig. 4.

TABLE II. Electron densities, bandwidths, and chemical potentials for the Yukawa parameters in Table I.

	A(LDF)	A(NLDF)	A(HF)	B(LDF)	B(NLDF)	B(HF)	C(LDF)	C(NLDF)	C(HF)
$10^3n(G_{110})$	1.488	1.342	1.348	1.610	1.416	1.441	1.741	1.488	1.557
$10^3n(G_{200})$	0.301	0.247	0.248	0.347	0.275	0.281	0.399	0.306	0.324
$10^3n(G_{211})$	0.107	0.085	0.087	0.124	0.094	0.098	0.143	0.105	0.115
$\mu-\epsilon_{k=0}$	0.3557	0.5366	0.5417	0.3472	0.6169	0.6251	0.3372	0.7584	0.7634
$\mu-\mu^{\mathrm{HF}}$	0.0078	−0.0055	···	0.0115	−0.0117	···	0.0116	−0.0071	···

cal than the indicated Fermi surface[15-17]. But because the Fermi surface of Li has not been measured with sufficient accuracy the quantitative aspects of the NLDF approximation were unresolved. The present results indicate that the NLDF approximation should not be expected to lead to precise predictions of the Fermi surface and therefore, these results are consistent with the Fermi surface of Li being considerably more distorted than the NLDF prediction.[1] However, it is unlikely that NLDF and LDF predicted Fermi surfaces would bear precisely the same relationship to the Fermi surface as they do to the HF Fermi surface shown in Figs. 4–6 since no set of Yukawa parameters leads to a self-energy which has all of the characteristics of a realistic self-energy.

Referring to Table II we see that, in contrast to the Fermi surface, the NLDF electron density is much closer to the HF electron density than is the LDF electron density. This is true even in set A in which all three Fermi surfaces are almost the same. Although the LDF electron density is not as accurate as the NLDF electron density, it is adequate for many purposes. The density functional theory[10-12] results in approximations to the self-energy that depend only on the electron density. Instead of solving the problem self-consistently the LDF charge density could be used to construct the self-energy and solve the problem non-self-consistently as has been done in several previous calculations.[1,13,14,23] We examine this approximation by comparing the NLDF self-consistent Fermi surfaces of Figs. 4–6 with non-self-consistent NLDF Fermi surfaces where $M_{\vec{r}}^{\mathrm{NL}}$ is a function of the LDF charge density. The latter are less than 5% of $\delta_{\vec{r}}-\delta_{\vec{r}_{100}}$ larger than the former indicating that the LDF electron density is useful if used in this way. Over most of the unit cell volume, the HF, NLDF, and LDF densities are almost the same; they differ only near $\vec{r}=0$. This is why the LDF charge density can be used.

As expected both the LDF and NLDF chemical potentials are very close to the HF value with the NLDF values being slightly better. This gives us confidence that the LDF approximation can be used to obtain chemical potentials in real systems.

If the NLDF bandwidths, $\mu-\epsilon_{k=0}$, are examined, it is noted that the value is very close to the HF result. This shows that for $\vec{k}$ below the Fermi surface the NLDF approximation to the self-energy is accurate. This may not be true however, if the approximation to M_h is energy dependent and this fact is not taken into account.

Use of the NLDF approximation compared to use of the LDF approximation results in improved electron densities, chemical potentials, and bandwidths but not in improved Fermi surfaces. This result illustrates the statement made in the Introduction that the Fermi surface is very sensitive to the self-energy approximations and is shown to be more sensitive than other properties. Such sensitivity can be understood by noting that the electron density and chemical potential are average properties since they involve integrals over occupied $\vec{k}$ space of energies and wave functions; on the other hand, the Fermi-surface distortions are intimately related to the changes in the self-energy when the direction of $\vec{k}$ is changed, with $|\vec{k}|$ near the Fermi surface. Thus a Fermi-surface calculation sets a standard of accuracy against which an approximation to the self-energy can be judged.

In summary we have shown that the nonlocal aspect of the self-energy operator is essential to obtain precise theoretical values of the Fermi surface. But on the basis of our model calculation it has not been shown that the NLDF approximation is more accurate than the LDF approximation for the calculation of Fermi surfaces. We have reconciled previous Fermi surface calculations with experiment in that our exact model Fermi surface is bracketed by the NLDF and LDF approximate Fermi surfaces as has been indicated in the alkali metals.

ACKNOWLEDGMENTS

We wish to thank W. R. Fehlner, A. E. Jacobs, M. Rasolt, and L. J. Sham for stimulating discussions and useful comments.

*Supported in part by the National Research Council of Canada and the Walter C. Sumner Foundation.

†Based on work submitted by S. B. Nickerson in partial fulfillment of the requirements for the degree of Doctor of Philosophy at the University of Toronto.

[1]M. Rasolt, S. B. Nickerson, and S. H. Vosko, Solid State Commun. 16, 827 (1975).
[2]L. Dagens and F. Perrot, Phys. Rev. B 8, 1281 (1973).
[3]S. T. Inoue, S. Asano, and J. Yamashita, J. Phys. Soc. Jpn. 30, 1546 (1971); 31, 422 (1971).
[4]J. F. Janak, A. R. Williams, and V. L. Moruzzi, Phys. Rev. B 6, 4367 (1972).
[5]M. J. G. Lee, Crit. Rev. Solid State Sci. 2, 83 (1971).
[6]J. Perdew and S. H. Vosko, J. Phys. F 4, 380 (1974).
[7]A. MacDonald and S. H. Vosko, J. Low Temp. Phys. (to be published).
[8]W. Y. Ching and J. Callaway, Phys. Rev. B 9, 5115 (1974).
[9]M. J. Lawrence, J. Phys. F 1, 836 (1971).
[10]L. J. Sham and W. Kohn, Phys. Rev. 145, 561 (1966).
[11]W. Kohn and L. J. Sham, Phys. Rev. 140, A1133 (1965).
[12]P. Hohenberg and W. Kohn, Phys. Rev. 136, B864 (1964).
[13]M. Rasolt and S. H. Vosko, Phys. Rev. Lett. 32, 297 (1974).
[14]M. Rasolt and S. H. Vosko, Phys. Rev. B 10, 4195 (1974).
[15]D. L. Randles and M. Springford, J. Phys. F 3, L185 (1973); and unpublished.
[16]J. J. Donaghy and A. T. Stewart, Phys. Rev. 164, 391 (1967).
[17]J. J. Paciga and D. L. Williams, Can. J. Phys. 49, 3227 (1971).
[18]B. Y. Tong and L. J. Sham, Phys. Rev. 144, 1 (1966).
[19]L. Hedin, Phys. Rev. 139, A796 (1965).
[20]A. L. Fetter and J. D. Walecka, *Quantum Theory of Many-Particle Systems* (McGraw-Hill, New York, 1971).
[21]W. R. Fehlner, S. B. Nickerson, and S. H. Vosko, Solid State Commun. 19, 83 (1976); W. R. Fehlner and S. H. Vosko, Can. J. Phys. (to be published).
[22]F. C. von der Lage and H. A. Bethe, Phys. Rev. 71, 612 (1947).
[23]G. Arbman and A. von Barth, J. Phys. F 5, 1155 (1975).